Performance Evaluation of Multipassage Tubes for Laminar Flow Applications

H. M. Soliman*
University of Manitoba, Winnipeg, Manitoba, Canada

The pressure drop and heat-transfer characteristics of multipassage tubes during fully developed, laminar, forced convection are investigated theoretically. Correlations were developed for the friction factor and for Nusselt number corresponding to two limiting thermal boundary conditions. Results are presented for a wide range of geometrical parameters from which it is seen that the friction factor and Nusselt number always exceed their respective value for smooth tubes. The performance of multipassage tubes is compared to that of smooth tubes and the objective functions for six different comparison scenarios were developed. Results of these comparisons show that although multipassage tubes are not effective in reducing the frontal (flow) area, they can produce substantial increases in heat transfer per unit pumping power at the same weight and significant reductions in weight at the same heat duty and pumping power. These gains are shown to be quite sensitive to the geometrical parameters.

Nomenclature

A = surface area (PL)
A_c = cross-sectional flow area
c_p = specific heat
D_h = hydraulic diameter ($4A_c/P$)
D_i = innermost diameter
D_o = outermost diameter
D_s = diameter of smooth tube
f = friction factor
h = mean heat-transfer coefficient
j = Colburn heat-transfer modulus
k = thermal conductivity
L = tube length
M_F = number of fins in each finned layer
M_L = number of finned layers
N = total number of parallel passages
Nu = Nusselt number
P = wetted perimeter
p = pressure
Pr = Prandtl number
q = heat input per unit length
Re = Reynolds number
T_b = bulk temperature
T_w = wall temperature
V = volume of tube material
W = mass flow rate
x = axial distance

Greek Symbols

β = pumping power
γ = dimensionless parameter defined by Eqs. (16b) and (17b)
Δp = total pressure drop
μ = dynamic viscosity
ρ = fluid density

Subscripts

D_o = quantity based on the outermost diameter
i = value for stream number i
in = at inlet of tube
out = at outlet of tube
s = value for smooth tube

Received June 30, 1988; revision received Nov. 7, 1988.

*Professor, Department of Mechanical Engineering.

I. Introduction

THE thermal effectiveness of tubular heat exchangers, in which the convective resistance on the inner surface of the tube constitutes the main barrier to heat flow, can be substantially increased by a number of augmentative techniques. Twisted-tape inserts, surface roughness, and internal finning are among the techniques that received considerable attention due to their simplicity and heat-transfer effectiveness. Normally, the increase in heat transfer over smooth-tube conditions is accompanied by increases in weight, pressure drop, and pumping power for the same tube length and mass flow rate. Consequently, performance evaluations are necessary in order to determine the optimum configuration of augmented tubes for a particular application by maximizing the appropriate objective function (as shown later).

One type of augmented tubes is the multipassage tubes, examples of which are shown schematically in Figs. 1a and 1b. These tubes are being manufactured by mechanically coupling a number of open-core internally finned tubes (Fig. 1c) such that intimate metal-to-metal contact is maintained between the fin tips of any tube and the outer surface of the tube next in size.[1] Thus, the fluid flowing through the pipe is subdivided into a large number of parallel streams each surrounded by wall surfaces at which heat transfer and frictional pressure drop take place.

Experimental results reported so far indicate that multipassage tubes are capable of superior performance compared to open-core internally finned tubes and smooth tubes. A major portion of the available data was reported by Carnavos[1] who explored the performance of five multipassage tubes with different core designs for cooling of a turbulent airstream. When comparing the multipassage tubes to smooth tubes at the same heat duty and pumping power, Carnavos concluded that reductions in tube length by a factor ranging from 2–10 (depending on core design) are possible with multipassage tubes. Another comparison based on similar pumping power and tube length showed that multipassage tubes can increase the heat-transfer rate over that of smooth tubes by a factor ranging from 1.7–10. These results are consistent with those of Soliman and Feingold[2] who compared the performance of a multipassage tube to those of an open-core internally finned tube and a smooth tube during cooling of an oil stream in laminar and transitional flows. The multipassage tube gave the best performance with a reduction in length by a factor of up to 10 compared to the smooth tube at the same mass flow rate and heat duty. Hilding and Coogan[3] reported data on the pressure drop and heat-transfer characteristics of 10 different

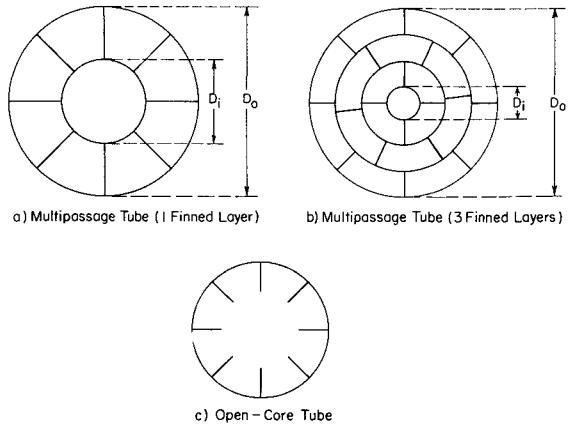

Fig. 1 Geometry.

internally finned tubes, of which only one can be classified as a multipassage tube. They showed that significant enhancements are possible, particularly in the laminar flow region. However, comparative evaluations of the performances of different tubes were not reported.

So far, there has been no theoretical studies reported on the basic characteristics and performance evaluation of multipassage tubes. The experimental studies indicate that core design is a major influencing factor. However, it is virtually impossible to experimentally test all possible designs due to the obvious prohibitive costs. The objectives of the present investigation are to determine theoretically the pressure drop and heat-transfer characteristics of multipassage tubes during fully developed, laminar, forced convection and to conduct performance evaluations of these tubes based on different objective functions in order to address different applications. A wide range of geometries is covered in order to provide some guidance on the selection of the most effective core design for each application.

II. Analysis

A. Idealizations

The following conditions and simplifying assumptions were adopted in carrying out the present analysis:

1) Fully developed laminar flow with constant heat-transfer coefficient and friction factor is assumed along each of the passages. In practice, developing flow is expected to exist for some entrance length in each passage. However, in view of the small hydraulic diameter of these passages relative to the tube diameter, this developing length is expected to amount only to a few tube diameters.

2) Entrance and exit losses are insignificant compared to frictional losses.

3) Fluid properties are treated as constants throughout all passages of the tube. Therefore, the present results are not recommended to cases with very large temperature difference between the inlet and exit of the tube.

4) Heat input to the tube is uniform in the axial (flow) direction.

5) Perfect bond (i.e., no thermal resistance) exists between fin tips and the outside surface of the next tube.

6) Pure forced convection is assumed within the passages, i.e., negligible free convective effects. This is justified by the fact that, in most applications, small Grashof numbers are expected in these passages due to their small hydraulic diameters.

B. Pressure Drop

With common inlet and outlet sections, it can be easily seen that the flow through the tube is subdivided into a number N of parallel streams such that the pressure gradient is the same for all passages and equal to the overall pressure gradient for the tube, i.e.,

$$\left(\frac{dp}{dx}\right)_i = \frac{dp}{dx} = \text{constant}, \qquad 1 \le i \le N \tag{1}$$

Also, the overall mass flow rate can be expressed as

$$W = \sum_{i=1}^{N} W_i \tag{2}$$

Defining the friction factor and Reynolds number (for a single passage or for the whole tube) by

$$f = \frac{\rho A_c^2 D_h}{2W^2}\left(-\frac{dp}{dx}\right) \tag{3a}$$

and

$$Re = WD_h/A_c\mu \tag{3b}$$

Consequently,

$$fRe = \frac{\rho A_c D_h^2}{2W\mu}\left(-\frac{dp}{dx}\right) \tag{3c}$$

Substituting Eq. (3c) into Eq. (2) and imposing the condition of Eq. (1), we get

$$fRe = \left[\sum_{i=1}^{N} \frac{1}{(fRe)_i}\left(\frac{D_{hi}}{D_h}\right)^2 \frac{A_{ci}}{A_c}\right]^{-1} \tag{4}$$

Thus, the overall fRe based on the hydraulic diameter of the tube can be easily evaluated from Eq. (4) using $(fRe)_i$ for the different passages. It is often preferable to present the overall results in terms of the outermost diameter in order to make the comparison with smooth tubes readily visible. In this case, the product fRe based on the outermost diameter D_o can be calculated from

$$(fRe)_{D_o} = fRe(D_o/D_h)^2 \tag{5}$$

Finally, the mass distribution among different streams, which is based on Eq. (1), can be evaluated from the following relation:

$$\frac{W_i}{W} = \frac{fRe}{(fRe)_i}\left(\frac{D_{hi}}{D_h}\right)^2 \frac{A_{ci}}{A_c} \tag{6}$$

C. Heat Transfer

The manner in which the overall heat transfer is distributed among the different passages of the tube can be very complicated if a generalized analysis of the problem is desired. This will involve simultaneous conduction in the solid walls of the core and convection in each of the N parallel streams, which amounts to a conjugated heat-transfer problem with a very complicated boundary. Although solution of such a problem is possible, numerical analysis is necessary and the associated computing costs can be very high (see for example Ref. 4 for the simpler case of plate-fin ducts).

Fortunately, the problem can be simplified by considering some limiting conditions which can closely approximate the heat-transfer problem for many applications. Consider for example the situation where the input heat is generated by passing an electric current through the solid walls of the core. If the walls' material is highly conductive, then the temperature would be uniform throughout the solid core at any axial cross section and the wall temperature would vary only in the axial direction. This limiting condition is normally referred to as the H1 boundary condition[5] and it was shown (e.g., Ref. 4) to be quite accurate for aluminum or copper walls. On the other hand, if the walls' thermal resistance is high (due to very

small thickness or very small thermal conductivity), then the heat generated in the wall will be immediately dissipated to the adjacent fluid by convection resulting in a uniform heat flux at the fluid–solid interfaces both cross sectionally and axially (assuming uniform wall thickness in the solid core). This second limiting condition, referred to as the H2 boundary condition,[5] was used by London[6] and Shah and London[7] in analyzing multipassage heat exchangers. The fully developed axial temperature distributions in the fluid and the wall corresponding to both limiting conditions are shown in Fig. 2. In this figure, T_{bi} and T_{bj} denote the bulk temperature in arbitrary passages i and j, respectively, T_{wi} and T_{wj} denote the average wall temperature for arbitrary passages i and j, respectively, while T_b and T_w denote the average bulk and wall temperatures for the whole tube, respectively, at any axial distance. These temperature distributions are assumed to prevail after a short developing distance from the tube inlet.

The fully developed H1 case is characterized by

$$\frac{dT_{bi}}{dx} = \frac{dT_b}{dx} = \frac{dT_w}{dx} = \text{constant} \tag{7}$$

Also, the rate of heat transfer per unit length in passage i is given by

$$q_i = W_i c_p \frac{dT_{bi}}{dx} \tag{8}$$

whereas the overall rate of heat transfer per unit length is

$$q = W c_p \frac{dT_b}{dx} \tag{9}$$

From Eqs. (7–9), we can easily conclude that $q_i/q = W_i/W$;

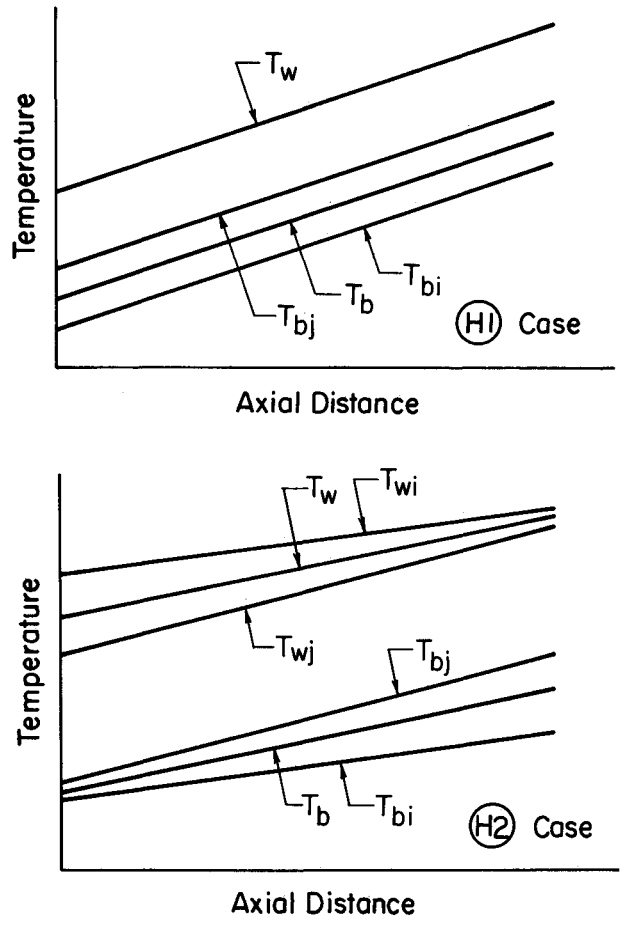

Fig. 2 Temperature distribution for the H1 and H2 boundary conditions.

i.e., input heat and input mass are distributed among the different flow passages in the same proportion. The wall-to-bulk temperature difference, shown schematically in Fig. 2, is governed by the following relation:

$$\frac{T_w - T_{bi}}{T_w - T_b} = \left(\frac{W_i}{W}\right)\left(\frac{h}{h_i}\right)\left(\frac{P}{P_i}\right) \tag{10}$$

Substituting the basic definition of Nusselt number, $Nu = hD_h/k$, we get

$$\frac{T_w - T_{bi}}{T_w - T_b} = \left(\frac{W_i}{W}\right)\left(\frac{D_{hi}}{D_h}\right)\left(\frac{P}{P_i}\right)\left(\frac{Nu}{Nu_i}\right) \tag{11}$$

Knowing that the overall wall-to-bulk temperature difference is given by

$$T_w - T_b = \sum_{i=1}^{N} \frac{W_i}{W}(T_w - T_{bi})$$

and substituting from Eq. (11), we obtain

$$Nu = \left[\sum_{i=1}^{N}\left(\frac{W_i}{W}\right)^2\left(\frac{D_{hi}}{D_h}\right)\left(\frac{P}{P_i}\right)\frac{1}{Nu_i}\right]^{-1} \tag{12}$$

Equation (12) provides a formula for the overall Nusselt number corresponding to the H1 boundary condition as a function of geometrical parameters, Nusselt numbers of different passages, and the mass distribution given by Eq. (6). It should be noted that Nu is independent of tube length, flow rate, or fluid properties.

In the H2 case, since the heat flux is uniform axially and circumferentially around the solid boundary of each passage, the total heat input at any tube cross section will be distributed among the N parallel streams in proportion to the perimeters of the passages, i.e.,

$$(q_i/q) = (P_i/P) \tag{13}$$

For any stream i, the bulk temperature and average wall temperature at any axial location x are given by

$$T_{bi} = T_{bi,\text{in}} + xq_i/(W_i c_p) \tag{14a}$$

and

$$T_{wi} = T_{wi,\text{out}} - q_i(L - x)/(W_i c_p) \tag{14b}$$

Therefore, the local wall-to-bulk temperature difference for stream i can be written as

$$T_{wi} - T_{bi} = (T_{wi,\text{out}} - T_{bi,\text{in}}) - \frac{q_i L}{W_i c_p} \tag{15}$$

Knowing that $q_i = h_i P_i (T_{wi} - T_{bi})$, $Nu_i = h_i D_{hi}/k$, and $Pr = \mu c_p/k$, Eq. (15) can be reduced to this form

$$\frac{T_{wi} - T_{bi}}{T_{wi,\text{out}} - T_{bi,\text{in}}} = \gamma_i \tag{16a}$$

where

$$\gamma_i = \frac{1}{1 + (4LNu_i/Re_i Pr D_{hi})} \tag{16b}$$

If we multiply both sides of Eq. (15) by W_i/W and perform the summation for all streams from $i = 1$ to $i = N$, keeping in mind that $q = \Sigma_{i=1}^{N} q_i$, we get (after reduction)

$$\frac{T_w - T_b}{T_{w,\text{out}} - T_{b,\text{in}}} = \gamma \tag{17a}$$

where

$$\gamma = \frac{1}{1 + (4LNu/RePrD_h)} \tag{17b}$$

From Eqs. (16a) and (17a), assuming that the variation in $T_{bi,\text{in}}$ and $T_{wi,\text{out}}$ among the different streams is small, we finally obtain

$$\gamma = \sum_{i=1}^{N} \frac{W_i}{W} \gamma_i \tag{18}$$

Substituting from Eqs. (16b) and (17b) into Eq. (18), the overall Nusselt number for the H2 boundary condition takes the following form:

$$Nu = \frac{RePrD_h}{4L} \cdot \frac{1 - \sum_{i=1}^{N} \left[\dfrac{W_i/W}{1 + \dfrac{4LNu_i}{Re_i PrD_{hi}}} \right]}{\sum_{i=1}^{N} \left[\dfrac{W_i/W}{1 + \dfrac{4LNu_i}{Re_i PrD_{hi}}} \right]} \tag{19}$$

The result given by Eq. (19) is surprising in that the overall Nusselt number for the multipassage tube is dependent on Reynolds and Prandtl numbers as well as the tube length even though the flow is assumed fully developed in all of the passages. For singly connected ducts (e.g., circular tubes, rectangular ducts, etc.), as well as the H1 case for the present geometry, Nu is independent of Re, Pr, and L. Shah and London[7] followed the ε–NTU approach in analyzing heat exchangers with parallel passages and obtained a formula [Eq. (600) of Ref. 7] which can be rearranged to a form identical to Eq. (19) by simple algebraic manipulation. The overall Nusselt numbers given by Eqs. (12) and (19) are based on the hydraulic diameter of the tube. In order to calculate the corresponding value based on the outermost diameter, this simple relation can be used

$$Nu_{D_o} = Nu(D_o/D_h)^2 \tag{20}$$

D. Performance Evaluation

The laminar, fully developed flow in smooth tubes is characterized by $(fRe)_s = 16$ and $Nu_s = 48/11$ for both the H1 and H2 cases. For multipassage tubes, both $(fRe)_{D_0}$ and Nu_{D_0} are expected to exceed their corresponding values for smooth tubes irrespective of core design. It becomes important then to determine under which scenarios would the multipassage tubes be preferable to smooth tubes and which are the optimum core designs. These decisions are guided by different performance criteria designed to suit various industrial applications as discussed in Refs. 8 and 9. In the present investigation, the pressure drop and heat-transfer performances of a multipassage tube (length L, outermost diameter D_o, and total mass flow rate W) are compared with those of a smooth tube (length L_s, diameter D_s, and mass flow rate W_s) on a one-to-one basis assuming similar fluid properties. Questions related to manufacturing cost, fouling, ease of cleaning, and maintenance are avoided here and the comparison is solely based on heat duty, pumping power, and material volume.

Based on the definitions stated earlier, the heat duty hA can be formulated as

$$hA = (4NuLWc_p/PrReD_h) \tag{21}$$

Therefore,

$$\frac{hA}{(hA)_s} = \frac{Nu}{Nu_s} \frac{L}{L_s} \frac{W}{W_s} \frac{Re_s}{Re} \frac{D_s}{D_h} \tag{22}$$

Substituting for the Reynolds-number ratio, we get

$$\frac{hA}{(hA)_s} = \frac{Nu}{Nu_s} \frac{L}{L_s} \left(\frac{D_s}{D_h}\right)^2 \frac{A_c}{A_{cs}} \tag{23}$$

Neglecting the reduction in flow area due to core material, i.e., assuming $A_c/A_{cs} = (D_o/D_s)^2$, Eq. (23) simplifies to

$$\frac{hA}{(hA)_s} = \frac{Nu_{D_o}}{Nu_s} \frac{L}{L_s} \tag{24}$$

The pumping power β is given by

$$\beta = \frac{W\,\Delta p}{\rho} = \frac{4\mu W^2 LfRe}{\rho^2 A_c D_h^2} \tag{25}$$

which, after reduction, results in

$$\frac{\beta}{\beta_s} = \left(\frac{W}{W_s}\right)^2 \frac{L}{L_s} \frac{(fRe)_{D_o}}{(fRe)_s} \left(\frac{D_s}{D_o}\right)^4 \tag{26}$$

Finally, the material volume used in manufacturing a tube (smooth or multipassage) is proportional to the wetted perimeter times the length, assuming uniform thickness throughout the solid. Thus,

$$\frac{V}{V_s} = \frac{P}{P_s} \frac{L}{L_s} \tag{27}$$

Equation (27) can be reformulated into

$$\frac{V}{V_s} = \frac{L}{L_s} \frac{D_o}{D_h} \frac{D_o}{D_s} \tag{28}$$

We now have Eqs. (24), (26), and (28) for the evaluation of the relative performance (multipassage to smooth). These three equations contain six unknown parameters, L/L_s, W/W_s, D_o/D_s, $hA/(hA)_s$, β/β_s, and V/V_s. Therefore, three parameters need to be specified according to the type of application at hand and the remaining three parameters can be easily evaluated. Table 1 lists the objective functions for six different ways (or scenarios) of comparison; all corresponding to equal pumping power, $\beta = \beta_s$. Cases A, B, C, and F explore the possibility of increased heat duty, while cases D and E explore the possibility of material saving at equal heat duty and pumping power. Results of these comparisons are presented and discussed later.

A parameter that is often used in evaluating the performance of enhanced surfaces is the "area goodness factor," j/f.[7] This parameter is defined by

$$j/f = NuPr^{-1/3}/fRe \tag{29}$$

Substituting for the dimensionless parameters in Eq. (29), we get

$$j/f = \frac{Pr^{2/3}}{2\rho c_p} \frac{W}{A_c^2} \frac{hA}{\Delta p} \tag{30}$$

It is evident from Eq. (30) that j/f represents the heat duty per unit pressure drop for the same W, A_c, and fluid properties. Since it is inversely proportional to A_c^2, it may also be regarded as a measure of the frontal (flow) area when the remaining parameters are kept constant. A closer examination reveals that a comparison based on j/f is really identical to case C of Table 1 since both provide a measure of the heat duty hA for equal flow area, flow rate, and pressure drop.

III. Results and Discussion

A. Geometrical Considerations

There is practically an infinite number of ways for designing the core of multipassage tubes. In this investigation, an at-

Table 1 Summary of objective functions ($\beta/\beta_s = 1$)

Case	D_o/D_s	L/L_s	W/W_s	V/V_s	$hA/(hA)_s$
A	1	1	$[(fRe)_s/(fRe)_{D_o}]^{1/2}$	D_o/D_h	Nu_{D_o}/Nu_s
B	$[(fRe)_{D_o}/(fRe)_s]^{1/4}$	1	1	$\frac{D_o}{D_h}\left[\frac{(fRe)_{D_o}}{(fRe)_s}\right]^{1/4}$	Nu_{D_o}/Nu_s
C	1	$(fRe)_s/(fRe)_{D_o}$	1	$\frac{D_o}{D_h}\frac{(fRe)_s}{(fRe)_{D_o}}$	$\frac{Nu}{Nu_s}\cdot\frac{(fRe)_s}{fRe}$
D	$\left[\frac{Nu_s}{Nu}\frac{fRe}{(fRe)_s}\right]^{1/4}$	Nu_s/Nu_{D_o}	1	$\frac{D_o}{D_h}\frac{Nu_s}{Nu_{D_o}}\left[\frac{Nu_s}{Nu}\frac{fRe}{(fRe)_s}\right]^{1/4}$	1
E	1	Nu_s/Nu_{D_o}	$\left[\frac{Nu}{Nu_s}\frac{(fRe)_s}{fRe}\right]^{1/2}$	$\frac{D_o}{D_h}\frac{Nu_s}{Nu_{D_o}}$	1
F	$\left[\frac{D_h}{D_o}\frac{(fRe)_{D_o}}{(fRe)_s}\right]^{0.2}$	$\left(\frac{D_h}{D_o}\right)^{0.8}\left[\frac{(fRe)_s}{(fRe)_{D_o}}\right]^{0.2}$	1	1	$\frac{Nu_{D_o}}{Nu_s}\left(\frac{D_h}{D_o}\right)^{0.8}\left[\frac{(fRe)_s}{(fRe)_{D_o}}\right]^{0.2}$

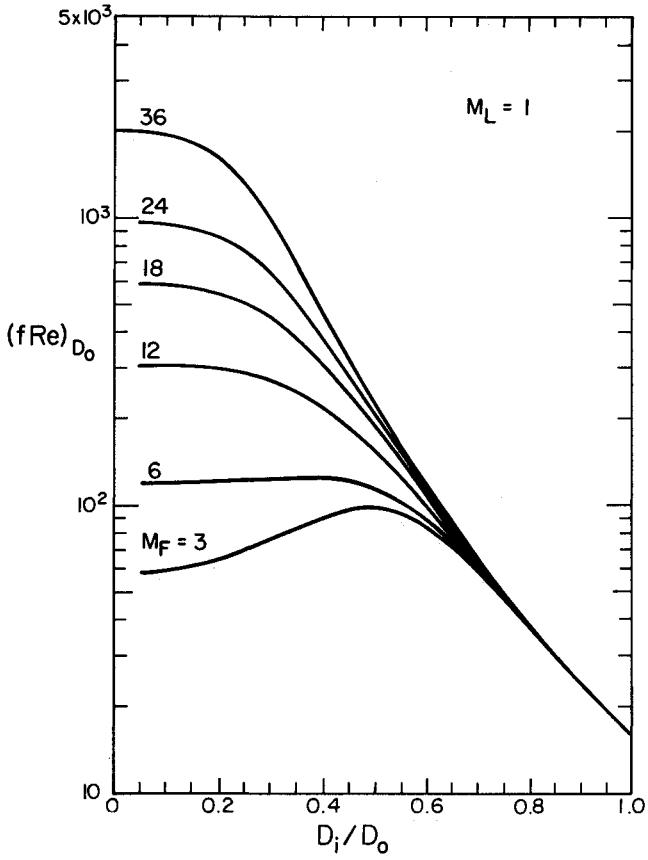

Fig. 3 Values of $(fRe)_{D_o}$ for $M_L = 1$.

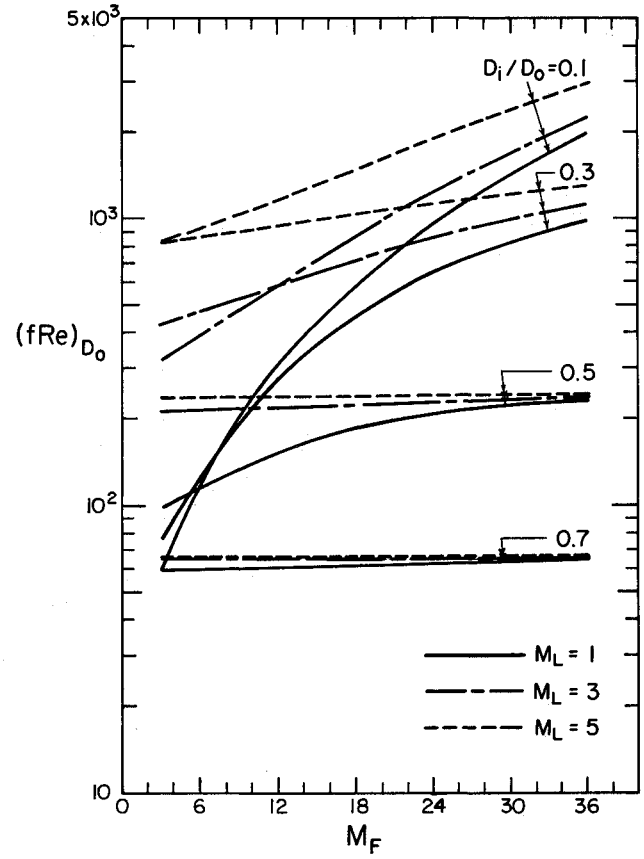

Fig. 4 Influence of M_L on $(fRe)_{D_o}$.

tempt was made to limit the number of geometrical parameters necessary to describe the core in order to facilitate the generation of results which are representative of the performance of these tubes. This was done by first assuming that the material forming the core is of negligible thickness. Each tube has an innermost smooth core of diameter D_i and an outermost diameter D_o with a number of finned layers M_L each having the same radial span between the two diameters. All finned layers of a given tube have the same number of fins M_F which are radial and straight in the axial (flow) direction. Thus, the geometry is completely defined by the three dimensionless parameters D_i/D_o, M_L, and M_F. Results were obtained for the following geometrical range: $0 < D_i/D_o < 1$; $M_L = 1$, 3, and 5; and $3 \le M_F \le 36$.

B. Pressure Drop

Equations (4) and (5) were used for the evaluation of $(fRe)_{D_o}$. The flow cross section consists of $(M_L \cdot M_F)$ parallel annular sector passages and one innermost smooth core. The results reported in Ref. 7 and later confirmed in Ref. 10, were used for $(fRe)_i$ in the annular sectors.

The resulting values of $(fRe)_{D_o}$ for $M_L = 1$ are shown in Fig. 3, and the influence of M_L is illustrated in Fig. 4. As expected, $(fRe)_{D_o}$ exceeds the value of 16 for smooth tubes over the whole geometrical range. The influence of M_F is much more pronounced at low values of M_L and D_i/D_o, while at large D_i/D_o, the influence of M_F on $(fRe)_{D_o}$ is small because a higher proportion of the flow is squeezed out of the

annular layers and forced to flow in the innermost smooth core. At small M_F values, $(fRe)_{D_o}$ reaches a maximum at a certain value of D_i/D_o (e.g., $D_i/D_o = 0.5$ for $M_L = 1$ and $M_F = 3$) and the location of this maximum shifts to lower values of D_i/D_o as M_F increases. For any given combination of M_L and D_i/D_o, $(fRe)_{D_o}$ increases monotonically with M_F, and similarly, $(fRe)_{D_o}$ increases monotonically with M_L at fixed M_F and D_i/D_o.

C. Heat Transfer

Nusselt numbers for the H1 boundary condition were computed from Eqs. (12) and (20) using the results reported in Ref. 10 for Nu_i in the annular sector passages. Figure 5 shows the resulting values of Nu_{D_o} at $M_L = 3$ and the influence of M_L is illustrated in Fig. 6. Similar to the friction-factor results, the Nusselt number for all multipassage tubes exceeds the value of 4.364 for smooth tubes. For any given M_L, the magnitude of Nu_{D_o} initially increases with M_F, reaches a maximum, and then decreases with further increases in M_F. The location of this maximum shifts to lower M_F as D_i/D_o increases. Another optimum value is evident in Fig. 5 as Nu_{D_o} for a given M_F reaches a maximum at a particular D_i/D_o. The value of D_i/D_o at which this optimum occurs decreases as M_F increases. Figure 6 shows some interesting trends in the variation of Nu_{D_o} with M_L. At small D_i/D_o, the heat-transfer performance improves (particularly at small M_F) as M_L increases and the opposite is true at large D_i/D_o. For intermediate values (e.g., $D_i/D_o = 0.3$), $M_L = 3$ gives the highest performance and $M_L = 1$ gives the lowest performance at $M_F = 3$, while for $M_F > 9$, the highest performance is given by $M_L = 1$ and the lowest is given by $M_L = 5$. These results illustrate that the heat-transfer performance of multipassage tubes is very sensitive to core design.

The influence of the boundary condition on the heat-transfer results is shown in Fig. 7 for $M_L = 5$. Values of the Nusselt number for the H2 boundary condition were computed from Eqs. (19) and (20) using the results in Ref. 10 for Nu_i in the annular sector passages. According to Eq. (19), Nu_{D_o} is dependent on fluid properties, tube length, and Reynolds number, and the present results were computed for these conditions: $Pr = 7$, $L/D_o = 400$, and $Re_{D_o} = WD_o/(\mu A_c) = 1000$. It is interesting to note from Fig. 7 that the results for both boundary conditions follow similar trends of variation with M_F and D_i/D_o. At low D_i/D_o, values of Nu_{D_o} are higher for the H1 condition and this trend reverses as D_i/D_o increases. However, for the most part, the difference between the two sets of results is small. For this reason, as well as the fact that the H1 results are independent of Pr, L, and Re, it was decided to use the H1 values in carrying out the performance evaluation of multipassage tubes.

D. Performance Evaluation

Since both $(fRe)_{D_o}$ and Nu_{D_o} exceed their respective values for smooth tubes, it is necessary to define the geometrical and

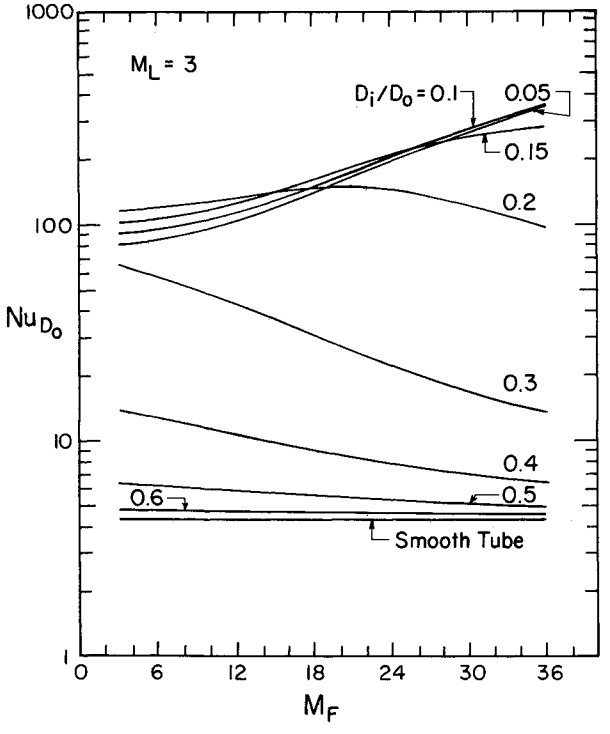

Fig. 5 Values of Nu_{D_o} for the H1 condition, $M_L = 3$.

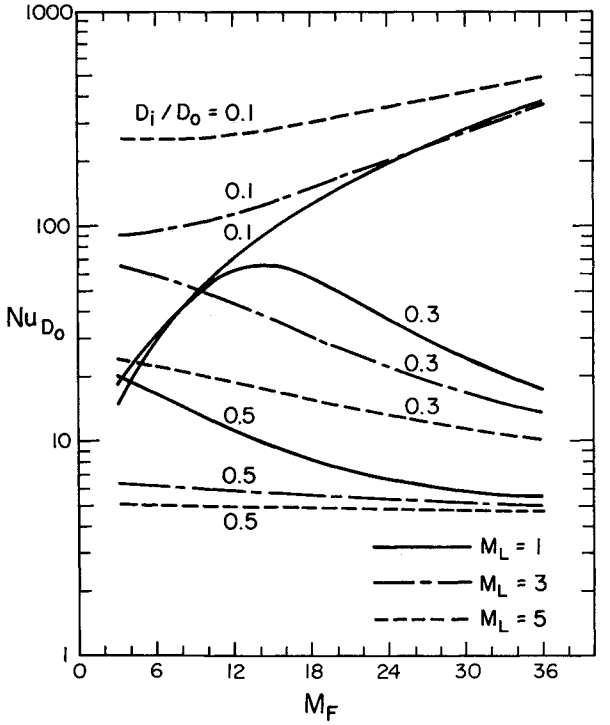

Fig. 6 Influence of M_L on Nu_{D_o} for the H1 condition.

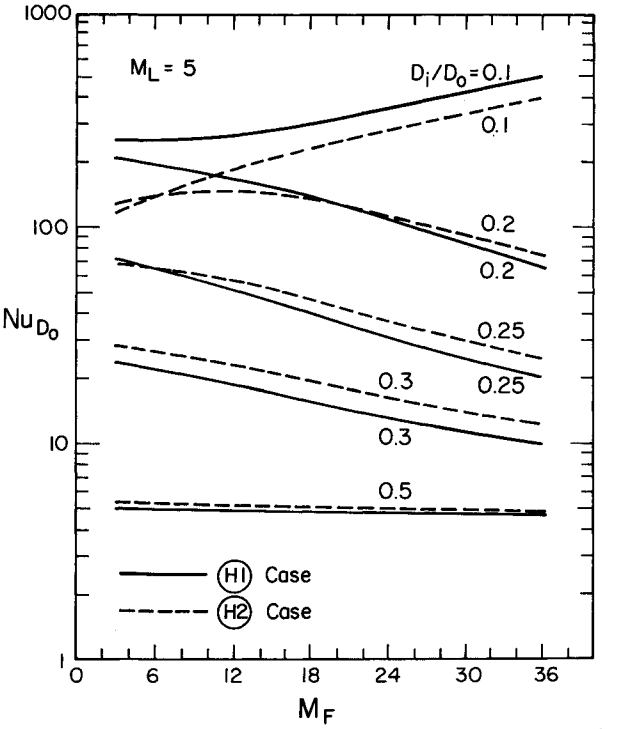

Fig. 7 Influence of boundary condition on Nu_{D_o}, $M_L = 5$. Results for the H2 condition correspond to $Pr = 7$, $L/D_o = 400$, and $Re_{D_o} = 1000$.

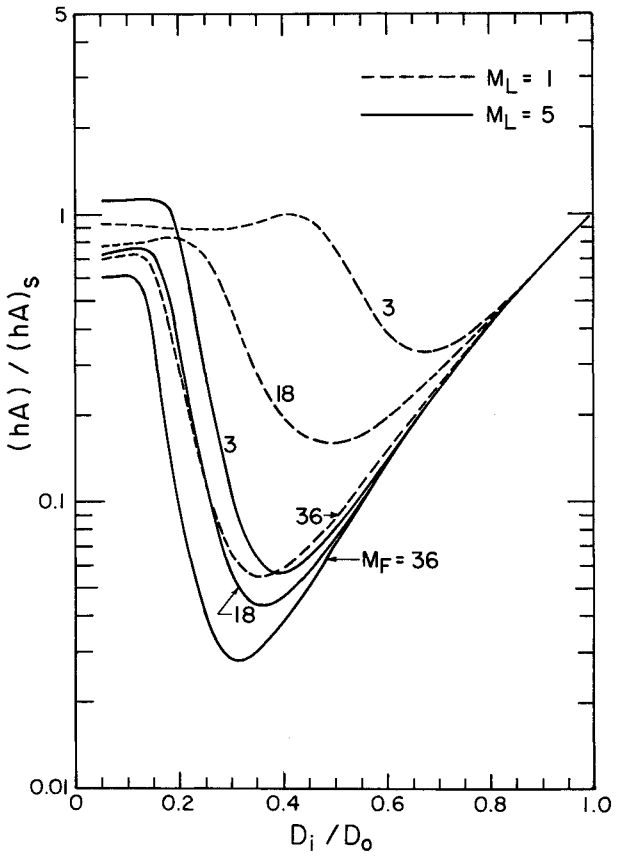

Fig. 8 Values of $hA/(hA)_s$ for case C, $M_L = 1$ and 5.

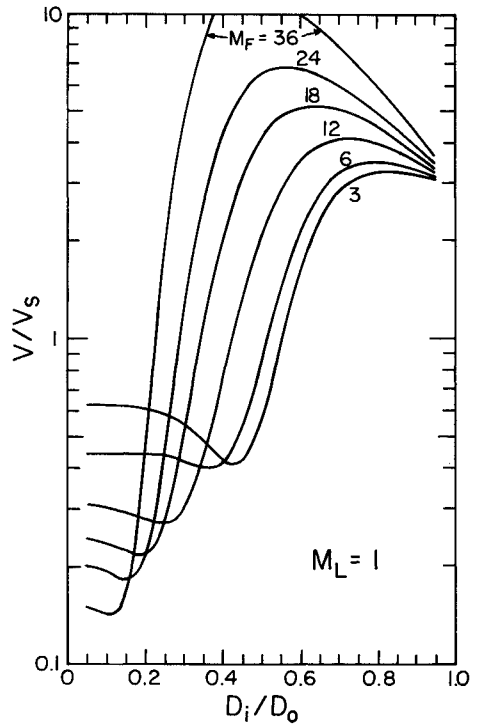

Fig. 9 Values of V/V_s for case D, $M_L = 1$.

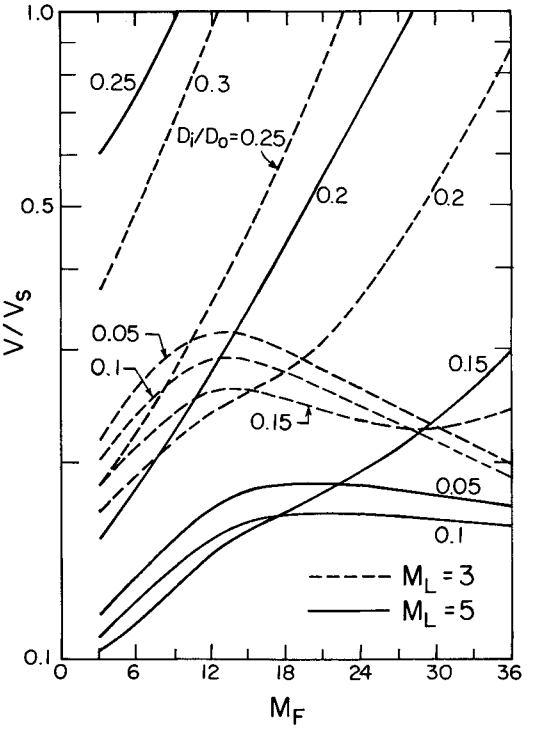

Fig. 10 Influence of M_L on V/V_s for case D.

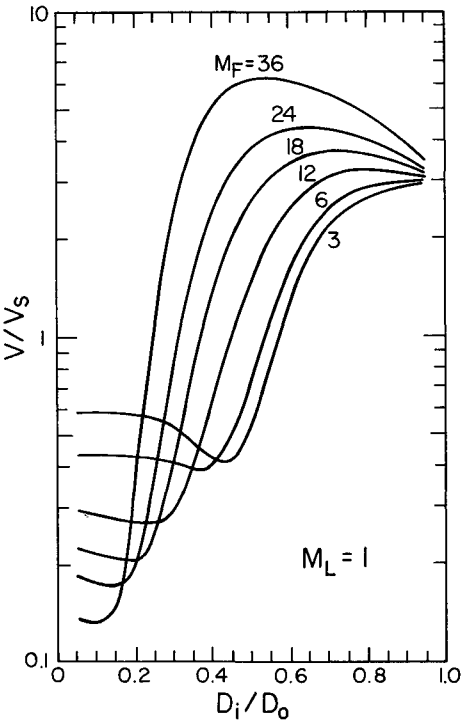

Fig. 11 Values of V/V_s for case E, $M_L = 1$.

flow conditions under which the performance of multipassage tubes may prove superior to smooth tubes. Six scenarios were identified earlier for this comparison, all corresponding to the condition of equal pumping power. The objective functions, on which the present comparisons are based, are listed in Table 1.

Case A involves a comparison of heat duty at the same basic geometry (outermost diameter and length) but reduced flow rate, whereas case B compares the heat duty at the same length and flow rate but increased diameter. In both cases, the heat duty is enhanced by a factor equal to the ratio of Nusselt numbers. However, this enhancement is achieved at the expense of increased material volume. Values of $hA/(hA)_s$ for cases A and B can be easily inferred from Figs. 5 and 6 from which it is evident that the most effective geometries are those with small D_i/D_o and large M_F.

In case C, multipassage tubes are compared to smooth tubes in terms of heat duty per unit pumping power at the same outermost diameter and mass flow rate. Figure 8 shows that multipassage tubes are generally inferior in this comparison with only marginal gains possible with $M_L = 5$, $M_F = 3$,

and $D_i/D_o < 0.18$. From the three comparisons presented so far, we learn that in order to achieve $hA/(hA)_s > 1$ at $\beta/\beta_s = 1$, we must impose $D_o/D_s > 1$ or $V/V_s > 1$.

In case D, the heat duty, pumping power, and mass flow rate are kept constant and the possibility of material saving is explored. These results are presented in Fig. 9 for $M_L = 1$, and the influence of M_L is shown in Fig. 10. This comparison is relevant to transportation and space applications where weight is an important factor. According to Figs. 9 and 10, weight reduction by a factor of up to 10 is possible with multipassage tubes depending on the geometry. A crucial factor in achieving this gain is D_i/D_o which must be kept low, particularly at high M_F. The optimum value of D_i/D_o depends on M_L and M_F. For example, at $M_L = 3$ and $M_F < 15$, the optimum value of D_i/D_o is 0.2, whereas for $M_L = 5$ and $M_F < 18$, the optimum value of D_i/D_o is 0.15. For $M_L = 1$, material saving is not possible beyond $D_i/D_o = 0.55$ and this upper limit decreases to 0.3 for $M_L = 3$ and 0.25 for $M_L = 5$. Finally, it is worthwhile to note that case D involves an increase in the frontal (flow) area, i.e., $D_o/D_s > 1$, and a decrease in tube length.

Case E is similar to case D except for maintaining equal diameter rather than equal flow rate. In this case, the mass flow rate must be decreased in order to maintain equal pumping power. The results in Figs. 11 and 12 show that material saving is possible and the trends of the results are similar to those shown in Figs. 9 and 10. The magnitude of reduction in the material is slightly higher in case E than case D.

In the final comparison (case F), the possibility of enhancing the heat duty at the same pumping power, flow rate, and material volume is explored. Figures 13 and 14 show that enhancements by a factor of up to 6 are possible. The trend in these results is similar to those of cases D and E in terms of the importance of selecting the appropriate D_i/D_o for each combination of M_L and M_F so that the maximum enhancement can be realized.

From the results of the above comparisons, it can be concluded that multipassage tubes can play an important role in the design of compact heat exchangers. Although these tubes may not be an attractive choice if a reduction in the frontal area of the heat exchanger is desired, increases in heat transfer per unit pumping power at the same weight and reductions in weight for the same heat duty and pumping power are possible. These gains are very sensitive to core design, and it is hoped that the present results will provide some guidance in selecting the optimum core design for various applications.

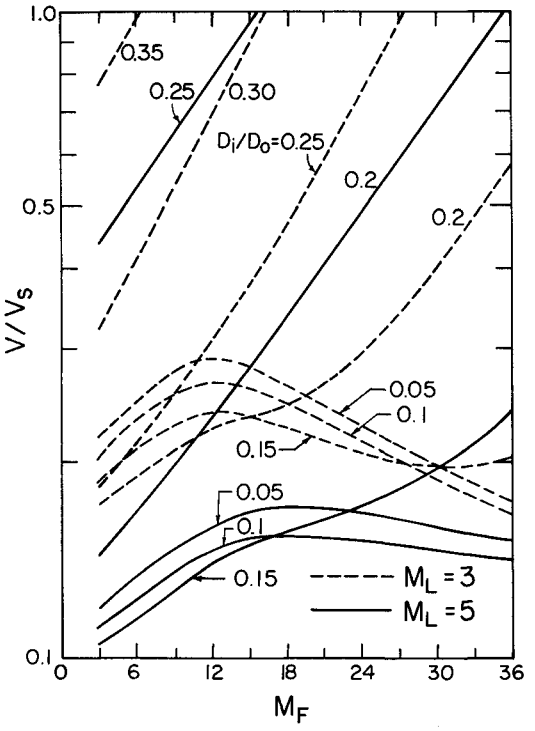

Fig. 12 Influence of M_L on V/V_s for case E.

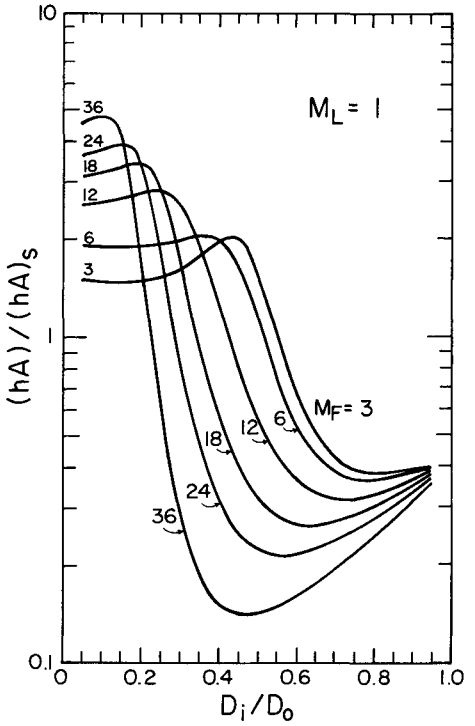

Fig. 13 Values of $hA/(hA)_s$ for case F, $M_L = 1$.

Acknowledgment

The financial assistance provided by the Natural Sciences and Engineering Research Council of Canada is gratefully acknowledged.

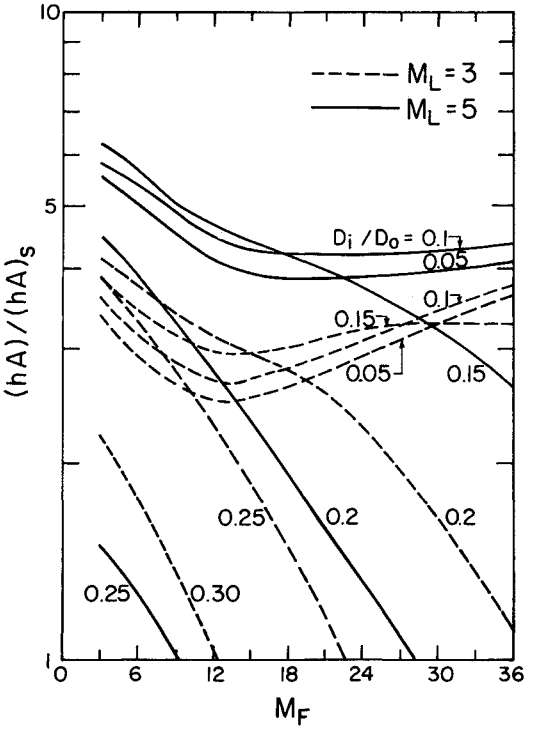

Fig. 14 Influence of M_L on $hA/(hA)_s$ for case F.

References

[1]Carnavos, T. C., "Cooling Air in Turbulent Flow with Multipassage Internally Finned Tubes," American Society of Mechanical Engineers, Paper 78-WA/HT-52, Dec. 1978.

[2]Soliman, H. M. and Feingold, A., "Heat Transfer, Pressure Drop, and Performance Evaluation of a Quintuplex Internally Finned Tube," American Society of Mechanical Engineers, Paper 77-HT-46, Aug. 1977.

[3]Hilding, W. E. and Coogan, C. H., Jr., "Heat-Transfer and Pressure Loss Measurements in Internally Finned Tubes," *Symposium on Air-Cooled Heat Exchangers*, American Society of Mechanical Engineers, National Heat-Transfer Conference, Cleveland, OH, Aug. 1964, pp. 57–85.

[4]Baliga, B. R. and Azrak, R. R., "Laminar Fully Developed Flow and Heat Transfer in Triangular Plate-Fin Ducts," American Society of Mechanical Engineers, Paper 84-HT-55, Aug. 1984.

[5]Shah, R. K. and London, A. L., "Thermal Boundary Conditions and Some Solutions for Laminar Duct Flow Forced Convection," *ASME Transactions, Journal of Heat Transfer*, Vol. 96, May 1974, pp. 159–165.

[6]London, A. L., "Laminar Flow Gas Turbine Regenerators—The Influence of Manufacturing Tolerances," *ASME Transactions, Journal of Engineering for Power*, Vol. 92, January 1970, pp. 46–56.

[7]Shah, R. K. and London, A. L., *Laminar Flow Forced Convection in Ducts*, Academic Press, New York, 1978.

[8]Webb, R. L., "Performance Evaluation Criteria for Use of Enhanced Heat-Transfer Surfaces in Heat Exchanger Design," *International Journal of Heat and Mass Transfer*, Vol. 24, April 1981, pp. 715–726.

[9]Trupp, A. C. and Soliman, H. M., "Performance Optimization of Internally Finned Tubes for Laminar Flow Heat Exchangers," *Heat Exchangers—Theory and Practice*, Hemisphere Publishing Corp., 1983, pp. 899–916.

[10]Soliman, H. M., "Laminar Heat Transfer in Annular Sector Ducts," *ASME Transactions, Journal of Heat Transfer*, Vol. 109, Feb. 1987, pp. 247–249.